

1 From local spectral species to global spectral  
2 communities: a benchmark for ecosystem  
3 diversity estimate by remote sensing

4 Duccio Rocchini<sup>1,2\*</sup>, Nicole Salvatori<sup>3,4</sup>, Carl Beierkuhnlein<sup>5</sup>,  
Alessandro Chiarucci<sup>1</sup>, Florian de Boissieu<sup>6</sup>, Michael Förster<sup>7</sup>,  
Carol X. Garzon-Lopez<sup>8</sup>, Thomas W. Gillespie<sup>9</sup>, Heidi C. Hauffe<sup>10</sup>,  
Kate S. He<sup>11</sup>, Birgit Kleinschmit<sup>7</sup>, Jonathan Lenoir<sup>12</sup>,  
Marco Malavasi<sup>2</sup>, Vítězslav Moudrý<sup>2</sup>, Harini Nagendra<sup>13</sup>,  
Davnah Payne<sup>14</sup>, Petra Šímová<sup>2</sup>, Michele Torresani<sup>15</sup>,  
Martin Wegmann<sup>16</sup>, Jean-Baptiste Féret<sup>6</sup>

5 November 4, 2020

6 <sup>1</sup> Alma Mater Studiorum University of Bologna, Department of Biologi-  
7 cal, Geological and Environmental Sciences, via Irnerio 42, 40126, Bologna,  
8 Italy

9 <sup>2</sup> Czech University of Life Sciences Prague, Faculty of Environmental Sci-  
10 ences, Department of Applied Geoinformatics and Spatial Planning, Kamýcká  
11 129, Praha - Suchbátka, 16500, Czech Republic

12 <sup>3</sup> University of Udine, Department of Agri-Food, Animal and Environ-  
13 mental Sciences (DI4A), via delle scienze 206, 33100 Udine (UD), Italy

14 <sup>4</sup> University of Trieste, Department of Life Sciences, via Giorgieri 5, 34100  
15 Trieste (TS), Italy

16 <sup>5</sup> Biogeography, BayCEER, University of Bayreuth, Universitätsstraße  
17 30, 95440 Bayreuth, Germany

18 <sup>6</sup> UMR-TETIS, IRSTEA Montpellier, Maison de la Télédétection, 500  
19 rue JF Breton, 34093, Montpellier Cedex 5, France

20 <sup>7</sup> Department of Geoinformation for Environmental Planning, Technical  
21 University of Berlin, Straße des 17. Juni 145, 10623 Berlin, Germany

22 <sup>8</sup> Ecology and Vegetation Physiology Group (EcoFiv), Universidad de los  
23 Andes, Cr. 1E No 18A, Bogotá, Colombia

24 <sup>9</sup> Department of Geography, University of California Los Angeles, Los  
25 Angeles, California 90095-1524, USA

26 <sup>10</sup> Fondazione Edmund Mach, Research and Innovation Centre, Depart-  
27 ment of Biodiversity and Molecular Ecology, Via E. Mach 1, 38010 S. Michele  
28 all'Adige (TN), Italy

29 <sup>11</sup> Department of Biological Sciences, Murray State University, Murray,  
30 KY 42071, USA

31 <sup>12</sup> UR "Ecologie et dynamique des systèmes anthropisés" (EDYSAN,  
32 UMR 7058 CNRS-UPJV), Université de Picardie Jules Verne, 1 Rue des  
33 Louvels, 80037 Amiens Cedex 1, France

34 <sup>13</sup> Azim Premji University, PES Institute of Technology Campus, Pixel  
35 Park, B Block, Electronics City, Hosur Road, Bangalore 560100, India

36 <sup>14</sup> University of Bern, Institute of Plant Sciences, GMBA office Altenber-  
37 grain 21, 3013 Bern, Switzerland

38 <sup>15</sup> Free University of Bolzano/Bozen, Faculty of Science and Technology,  
39 Piazza Università/Universitätsplatz 1, 39100, Bolzano, Bozen, Italy

40 <sup>16</sup> Department of Remote Sensing, Remote Sensing and Biodiversity Re-  
41 search Group, University of Wuerzburg, Wuerzburg, Germany

42

## Abstract

43 In the light of unprecedented change in global biodiversity, real-  
44 time and accurate ecosystem and biodiversity assessments are becom-  
45 ing increasingly essential. Nevertheless, estimation of biodiversity us-  
46 ing ecological field data can be difficult for several reasons. For in-  
47 stance, for very large areas, it is challenging to collect data that pro-  
48 vide reliable information. Some of these restrictions in Earth obser-  
49 vation can be avoided through the use of remote sensing approaches.  
50 Various studies have estimated biodiversity on the basis of the Spec-  
51 tral Variation Hypothesis (SVH). According to this hypothesis, spec-  
52 tral heterogeneity over the different pixel units of a spatial grid reflects  
53 a higher niche heterogeneity, allowing more organisms to coexist. Re-  
54 cently, the spectral species concept has been derived, following the  
55 consideration that spectral heterogeneity at a landscape scale corre-  
56 sponds to a combination of subspaces sharing a similar spectral signa-  
57 ture. With the use of high resolution remote sensing data, on a local  
58 scale, these subspaces can be identified as separate spectral entities,  
59 the so called "spectral species". Our approach extends this concept  
60 over wide spatial extents and to a higher level of biological organiza-  
61 tion. We applied this method to MODIS imagery data across Europe.  
62 Obviously, in this case, a spectral species identified by MODIS is not  
63 associated to a single plant species in the field but rather to a species

64 assemblage, habitat, or ecosystem. Based on such spectral informa-  
65 tion, we propose a straightforward method to derive  $\alpha$ - (local relative  
66 abundance and richness of spectral species) and  $\beta$ -diversity (turnover  
67 of spectral species) maps over wide geographical areas.

68 *Keywords:* biodiversity; ecological informatics; modelling; remote sens-  
69 ing; satellite imagery.

## 70 **1 Introduction**

### 71 **1.1 A quest for robust and reproducible $\alpha$ - and $\beta$ -** 72 **diversity measurement**

73 The variability of life on Earth is heterogeneously distributed across the  
74 planet; in fact, ecologists and biogeographers have long questioned the po-  
75 tential causes of biodiversity distribution. Recently, the speed of change and  
76 the uncertainty about possible consequences on biodiversity is concerning to  
77 the global scientific community. The perception of these processes trans-  
78 lates into the need to use standardized methods for biodiversity assessment  
79 and monitoring in order to gain a better understanding and identify general  
80 trends.

81 There is open debate as to the most reliable metrics for assessing biodiver-  
82 sity (see Jurasinski et al. (2009); Tuomisto (2010)). Until now, no consistent  
83 definition exists. Even the definition according to the Convention on Bi-  
84 ological Diversity (CBD, 1992, <https://www.cbd.int/convention/text/>)  
85 is more confusing than clear: “Biological Diversity means the variability  
86 among living organisms from all sources, including, inter alia, terrestrial,  
87 marine and other aquatic ecosystems and the ecological complexes of which  
88 they are part; this includes diversity within species, between species and of  
89 ecosystems.” Biodiversity obviously includes quantitative (number of species,  
90 alpha-diversity, gamma-diversity), qualitative (turnover, composition, beta-  
91 diversity) and functional (complexity, trophic levels, ecosystem services) as-  
92 pects. To sum up our understanding on the term biodiversity (i.e. biological  
93 diversity) and to base our study on a more general and consistent concept,  
94 “biodiversity characterizes qualitative, quantitative and functional aspects of  
95 biotic units at various levels of organization in a concrete or abstract con-  
96 text, and at a given temporal or/and spatial scale” (Beierkuhnlein, 2003). In  
97 consequence, species richness and metrics that are based on it are important,  
98 but they represent just one aspect of biodiversity. In fact, the total number  
99 of species co-occurring in a given community ( $\alpha$ -diversity) is nested within

100 the total number of a species pools occurring for instance at the landscape  
101 level ( $\gamma$ -diversity). But the reduction of biodiversity to the perspective of  
102 inventory and proportion would not cover spatial gradients in composition  
103 and species turnover (differentiation,  $\beta$ -diversity) (Jurasinski et al., 2009;  
104 Baselga, 2012) and also ignores functional diversity (e.g. functional traits),  
105 which is the main driver of ecosystem functioning.

106 In general,  $\beta$ -diversity is a crucial measure, since, given the same lo-  
107 cal richness of different sites ( $\alpha$ -diversity), it directly considers the turnover  
108 among them. As an example, let A and B be two sampling sites with 10  
109 different species each. If all 10 species are fully shared, the total  $\gamma$ -diversity  
110 would equal 10 species, while if all 10 species are completely different from  
111 one site to the other (high turnover, high  $\beta$ -diversity) the total diversity of  
112 the whole area based on the two focal sites would double.

113 Therefore, it becomes particularly interesting to understand how  $\beta$ -diversity  
114 originates, investigating how species composition differs among sites. In  
115 fact, species composition could be related to environmental conditions, or  
116 it could randomly fluctuate. A generally accepted hypothesis suggests that  
117  $\beta$ -diversity might change as a function of species types living in a certain  
118 community. For instance,  $\beta$ -diversity should be small when communities are  
119 dominated by a limited number of competitive species; this is recognized as  
120 the null hypothesis and it entails a uniform distribution in species composi-  
121 tion (Legendre et al., 2005).

122 The  $\beta$ -diversity concept reflects the environmental heterogeneity between  
123 sites and thus within a given larger area that contains several of the focal  
124 study sites. Heterogeneity is in fact highly associated with a high degree  
125 of biological diversity since heterogeneous sites offer a diversity of ecological  
126 niches (sensu Elton (1958)) that can be occupied if the species pool offers the  
127 respective ecological diversity to address these niches (Gaston, 2000; Rocchini  
128 et al., 2010). Furthermore, since  $\beta$ -diversity can be described as the spatial  
129 turnover among sites within a given region, it captures a fundamental feature  
130 of the spatial pattern of biodiversity.

131 In some cases, spatial turnover can result from local extinction processes  
132 that affect certain species more than others and enhance the dissimilarity  
133 between sites without dispersal (Steinitz et al., 2006). This is the case in  
134 highly fragmented landscapes where dispersal is limited (Hobbs et al., 2006).  
135 Even stochastic processes (sensu Moran (1950) and Clark (2008)) may en-  
136 hance  $\beta$ -diversity in previously homogeneous ecosystems. For instance, sud-  
137 den fragmentation (Alados et al., 2009) can lead to disfunctional source-sink  
138 metapopulations with intrinsic influences on the degree of spatial (and ge-  
139 netic) connectivity of organisms (Waples and Gaggiotti, 2006), resulting in  
140 the local loss of sink populations. However, in most situations, the spatial

141 turnover and therefore the dispersal of species between sites (metapopula-  
142 tion and metacommunity dynamics) is linked to the distance among sites.  
143 Strictly speaking, the similarity between two sites decays with increasing dis-  
144 tance between them (Rocchini, 2007), a process also known as the distance  
145 decay in similarity or the Tobler's first law of geography (Tobler, 1970).

146 Hence, modelling the distribution of  $\beta$ -diversity in space is based on  
147 softening the role of individual species, which are not even completely de-  
148 scribed at wide geographical scales, for the sake of estimating a more ef-  
149 ficient proxy for ecosystem patterns and processes. When these esti-  
150 mates are available from remote sensing data, this process can lead to rapid,  
151 large-scale monitoring and support management intervention aimed at pre-  
152 serving entire ecosystems, as stipulated by the Aichi Biodiversity Targets  
153 (<https://www.cbd.int/sp/>).

154 Field-based studies require an enormous investment in time in order  
155 to collect reliable biodiversity data. A pioneering example is the public  
156 database of the Global Biodiversity Information Facility (GBIF, <https://www.gbif.org/>). GBIF is a network funded by the world's governments  
157 which contains almost 41,000 databases of species occurrences spread out  
158 across the world. The large amount of publically accessible data and the  
159 available techniques to analyze them will certainly facilitate biodiversity as-  
160 sessment for the areas that it covers. Unfortunately, however, although it  
161 would be possible in principle to use these data to make reasonable assump-  
162 tions about biodiversity over larger areas, there are several limitations due  
163 to their quality (Maldonado et al., 2015). The errors that usually arise from  
164 field data are due to: (i) lack of or erroneous geographic coordinates of the  
165 sampling sites; (ii) incorrect taxonomic identification with poor quality con-  
166 trol; and (iii) difficulties in proving a reliable random sampling with large  
167 areas being poorly covered. Furthermore, these data often appear as point  
168 data, while grids are usually used in order to synthesize diversity metrics.  
169 In addition, these data are mainly collected from presence-only data with-  
170 out any link to relative abundance, dominance, biomass or cover, which in-  
171 stead, is reflected in remote sensing. Finally, GBIF data are inadequate for  
172 local estimates of biodiversity as they do not consider co-occurrence data.  
173 Indeed, and contrary to recent databases at the community level such as  
174 the European Vegetation Archive (EVA) (Chytry et al., 2016) or the sPlot  
175 initiative (Bruehlheide et al., 2019), GBIF does not provide information on  
176 species co-occurrence which is very problematic for biodiversity assessment  
177 and monitoring. Despite the disadvantages that come from the use of public  
178 databases, there is some benefits in the use of such data. First of all, there  
179 is a huge amount of data collected and provided by citizens and research  
180 institutions available in the GBIF database when compared to the data that  
181

182 could be collected locally, resulting in a huge saving of time and costs. More-  
183 over, GBIF data are standardized to the same format and therefore ready to  
184 use.

185 To overcome the issues due to the collection and availability of in situ  
186 ecological data, remote sensing imagery has become more and more impor-  
187 tant and is now considered a reliable tool to assess and monitor biodiversity  
188 (Tuanmu and Jetz, 2015).

## 189 1.2 The spectral species concept

190 Remote sensing based approaches have proven to be useful modelling tech-  
191 niques to detect the variability of biodiversity in space and time across scales  
192 of biological organisation, at different grains (spatial resolutions) and extents  
193 (Rocchini et al., 2013). Airborne sensors have even been used to detect and  
194 map single species distributions (Skorownek et al., 2017a), even the most  
195 tiny and inconspicuous ones such as *Campylopus introflexus*, a moss species  
196 which is highly invasive in Europe (Skorownek et al., 2017b).

197 Remote sensing techniques have been used to study the impact of land-  
198 scape and environment on biodiversity, and to explore and visualize spatial  
199 data and biodiversity change. Therefore, remote sensing data have become  
200 among the most time and cost effective tools, allowing to make relevant con-  
201 servation actions in a relatively short period of time. Furthermore, remote  
202 sensing demonstrated the impact of biodiversity (including non-native inva-  
203 sive species) on ecosystem functioning (Ewald et al., 2018).

204 In general, vegetation absorbs the blue and the red light, for photosyn-  
205 thesis, while it reflects near infrared (hereafter, NIR) radiation due to the  
206 physical structure of the cells composing the leaf mesophyllum (Wegmann  
207 et al., 2016). The bands relative to RED and NIR are used as proxies for  
208 photosynthetic activity of the vegetation. These bands are usually incor-  
209 porated in a widely used index, the normalized difference vegetation index  
210 (NDVI), which is calculated as  $NDVI = (NIR - RED) / (NIR + RED)$ . The higher  
211 the relative abundance of photosynthetic vegetation, the higher would be the  
212 reflectance in the NIR band and the absorption in the RED band. NDVI  
213 ranges from -1 to 1, with 0 values usually associated with non vegetated  
214 areas and negative values associated with water surfaces or snow.

215 This index has widely been used to discriminate different vegetation types  
216 over an area. In fact, in several studies, NDVI is positively correlated to the  
217 net primary productivity (NPP, e.g. Gillespie et al. (2008)). Therefore, it  
218 can be used as a proxy to quantify species richness and diversity, based on the  
219 species-energy theory, proposed by Currie (1991), namely a relation between  
220 species richness and energy, that would depend mainly on annual potential



221 evapotranspiration and actual evapotranspiration. Another hypothesis re-  
222 lated to the variability in space of the spectral signal has been proposed  
223 by Palmer et al. (2002). The so called spectral variation hypothesis (SVH)  
224 states that the higher the environmental heterogeneity the higher would be  
225 the species diversity of an area, due to a higher number of available ecological  
226 niches.

227 Hence, based on the SVH, spectral variability can effectively be related to  
228 environmental heterogeneity and therefore it could be used to assess species  
229 biodiversity of an area. In this sense, since the spectral variability is derived  
230 from the information present in the pixels of an acquired image, it is im-  
231 portant that the pixels, describing the area of study, would have a spatial  
232 resolution coherent with the ecological assumptions taken into account and  
233 such that predictions on biodiversity can be made.

234 Among the most novel methods to estimate diversity by remote sensing,  
235 described in Rocchini et al. (2018), the spectral species concept (Féret and  
236 Asner, 2014) is one of the most powerful, since it allows to couple k-means  
237 approaches to the gridded data obtained from remote sensing technologies  
238 as a mean to derive  $\alpha$ - and  $\beta$ -diversity 2D-matrices. The spectral species al-  
239 gorithm allows the separation of the spectral space in subunits identified as  
240 spectral species. Its root theory is built upon two major founding principles.  
241 The first is the aforementioned Spectral Variation Hypothesis, relating spec-  
242 tral to environmental heterogeneity. The second is based on the plant optical  
243 types proposed by Ustin and Gamon (2010). This concept is mainly related  
244 to the use of particular sensors providing high spatial resolution images and  
245 able to measure different signals about the phenology, the biochemistry and  
246 the structure of vegetation. Such sensors can obtain information at the in-  
247 dividual plant scale level.

248 The method is based on an unsupervised clustering algorithm, first rely-  
249 ing on dimensionality reduction obtained after running a principal component  
250 analysis (PCA) and then on the actual clustering of the pixels, with the sub-  
251 sequent assignment to spectral species, based on a k-means approach. PCA  
252 and similar clustering methods have already been shown to reliably reduce  
253 the multidimensional spectral sets for models on species and biodiversity  
254 distribution (Rocchini et al., 2010). Furthermore, the method provides an  
255 interesting visual inspection of diversity building  $\alpha$ - and  $\beta$ -diversity maps.

256 As far as we know, the spectral species concept has been applied so far  
257 only at the local scale (Féret and Asner, 2014). Hence, the aim of this  
258 manuscript is to extend this concept over wider spatial extents passing to a  
259 spectral community concept, by generating a heterogeneity map at a wide  
260 geographical scale to estimate  $\alpha$ - and  $\beta$ -diversity across Europe.

## 261 **2 The algorithm**

262 The spectral species algorithm was originally developed to map tropical forest  
263 canopy diversity using imaging spectroscopy with a spatial resolution up to  
264 2 meters (Féret and Asner (2014), Figure 1). Following the hypothesis that  
265 species are spectrally separable (Asner and Martin, 2009), the approach is  
266 based on the segmentation of the spectral space defined by the remote sensing  
267 data. In fact the spectral space is assumed to be a combination of several  
268 subspaces, reflecting the “signature” of one or several species. Therefore  
269 these subspaces would be the expression of a more general “spectral species”.  
270 From the resultant “spectral community”, it would be possible to derive the  
271 diversity of an area. Therefore, the output of this algorithm is not a list of  
272 the actual species of an area, but rather a map of the distribution of the  
273 spectral communities available within the area that may be used to calculate  
274 several diversity indices. In particular we focused here on  $\alpha$ - and  $\beta$ -diversity  
275 metrics. Both introduced by Whittaker (1972), the first reflects the mean  
276 species diversity in sites at a local scale whereas the second is an indicator  
277 of the spatial (or temporal) heterogeneity at a relatively larger scale. In the  
278 algorithm,  $\alpha$ -diversity is calculated in a neighbourhood (plot) of  $n \times n$  pixels  
279 by the Shannon diversity index (Shannon, 1948) calculated as follow:

$$H' = -\sum_{s=1}^N p_s \ln p_s \quad (1)$$

280 where  $p_s$  is the proportion of each spectral species  $s$  in each plot.

281 The  $\beta$ -diversity indicator is instead computed by the Bray-Curtis (here-  
282 after BC) dissimilarity metric (Bray and Curtis, 1957):

$$BC_{ij} = \frac{\sum_{s=1}^N |x_{is} - x_{js}|}{\sum_{s=1}^N (x_{is} + x_{js})} \quad (2)$$

283 where  $BC_{ij}$  is the dissimilarity between plots  $i$  and  $j$  and  $x_{is}$  and  $x_{js}$  are the  
284 abundances of spectral species  $s$  in plots  $i$  and  $j$ .

285 In the spectral species algorithm, once the BC dissimilarity matrix be-  
286 tween all pairs of plots is computed, a multidimensional scaling is performed  
287 in order to translate information about the pairwise dissimilarity among P  
288 plots into a configuration of P points mapped in a 3-dimensional Cartesian  
289 space such as NMDS or PCoA (Mead, 1992). This simplified translation of  
290 the BC dissimilarity matrix can then be displayed as a colored map. More  
291 details can be found in Féret and de Boissieu (in press).

292 While the Shannon index has a theoretical maximum limit corresponding  
293 to the  $\ln(\text{richness})$ , the Bray-Curtis index ranges from 0 to 1, where 0 is



294 indicating that the two sites are identical whereas 1 indicates that the two  
295 sites do not share species. Hence, BC can be considered as an estimate of  
296 the heterogeneity of a certain area. The final aim of the method was to gener-  
297 ate an heterogeneity map across the study region. Strictly speaking, the  
298 method is a clustering approach which (i) divides the subspaces in spectral  
299 units and (ii) assigns it to spectral species from which (iii) different diver-  
300 sity maps can be obtained. Box 1 focuses in detail on the main steps of  
301 the algorithm, while the dedicated R package `biodivMapR` is now available  
302 (<https://github.com/jbferet/biodivMapR>) and fully described in F eret and  
303 de Boissieu (in press).

## 304 2.1 Application of the algorithm

305 Remote sensing data are usually provided as raster objects with a geographic  
306 coordinate system information, namely regular grids (matrices) or stacks of  
307 raster layers (e.g. one raster layer per band for multispectral or hyperspectral  
308 data), in which each cell represents a pixel with the corresponding reflectance  
309 value associated to a specific band. Such data have been manipulated with  
310 the Software R Development Core Team (2019). R can be used for remote  
311 sensing data analysis since it includes spatial functionalities throughout a  
312 suite of R packages like the `rgdal` and `raster` packages (see Box 2 for more  
313 information).

314 Our main purpose was to apply the spectral species algorithm to a continental-  
315 scale geographical region such as Europe. Hence, Moderate Resolution Imag-  
316 ing Spectroradiometer (MODIS) data, with a spatial resolution of 500m cov-  
317 ering Europe, were downloaded from the United States Geological Survey  
318 (USGS) site (<https://lpdaac.usgs.gov/products/mod09a1v006/>). After  
319 a visual check of the images, in order to guarantee i) the coverage of a com-  
320 plete phenological period and to ii) avoid noise related to clouds, we referred  
321 to the RED and NIR bands from 2018 from January to December (one im-  
322 age per month), to calculate NDVI, by generating a sample set of 12 NDVI  
323 images (Figure 2).

324 Due to the coarse spatial resolution of MODIS images (500m), the re-  
325 flectance related to a single plant species is averaged and mixed with the  
326 reflectance of other species within a single pixel. In other words, the direct  
327 relationship between spectral species detected in the spectral space versus  
328 the number of plant species does not hold true. However, in any case, from a  
329 diversity measurement perspective, this is just a matter of terms being used,  
330 with spectral species being actually more related to field plant communities,  
331 habitats or other ecological entities.

332 For the derivation of spectral species, in order to define the number of

333 clusters, we relied on the highest number of clusters with stable results after  
334 a trial and error procedure, reaching 200 clusters, i.e. spectral species. Once  
335 pixels with similar NDVI values in 12 dimensions were clumped together,  
336 Shannon's  $H'$  was calculated with a window size of 10x10 pixels and an out-  
337 put resolution of 5km. The attained  $\alpha$ -diversity map quantitatively showed  
338 the local spectral diversity distribution over Europe (Figure 3), with a higher  
339 heterogeneity found in i) more topographically complex regions, mainly due  
340 to strong local differences induced by elevation gradients (passing from forests  
341 to grasslands, to rocks and snow), and/or differences in terms of seasonal-  
342 ity in relation with elevation, as in Rocchini et al. (2019), and in ii) more  
343 contrasted agricultural areas in both the spatial and temporal dimensions  
344 (Hobbs et al., 2006; Vihervaara et al., 2017). Concerning topographical com-  
345 plexity, the higher variability in areas with a marked topographical gradient  
346 might be related to shadows. Local field work in such areas will be needed  
347 to validate the measurements in such areas.

348  $\beta$ -diversity (Figure 3) showed a clear differentiation among different areas  
349 over Europe. The attained map was in line with the European Environmental  
350 Agency (EEA) map of ecoregions (Figure 4, see Mucher et al. (2009)). The  
351 correspondence of the achieved patterns in the two maps was apparent, with  
352 a similar contour of the major ecoregions such as the mediterranean, the  
353 atlantic, the continental, the boreal and the alpin regions. This demonstrates  
354 an intrinsic ability of the spectral species approach to capture differences  
355 in the physiological and functional properties of vegetation even at wide  
356 spatial scales, starting from spectral reflectance or spectral indices. Minor  
357 differences were mainly related to the biogeographical (i.e., purely spatial)  
358 differentiation of ecoregions in the EEA map. As an example, north and  
359 south alpine ecoregions could not be distinguished by the spectral species  
360 approach, since they both have very similar conifer species composition, with  
361 the same physiological, phenological and thus spectral pattern.

### 362 **3 Discussion**

363 In this paper, for the first time, the spectral species concept has been ex-  
364 tended from the consideration of a single species to an entire community.  
365 We demonstrated that the combined use of the novel unsupervised cluster-  
366 ing method proposed by Féret and Asner (2014) with NDVI time series at  
367 European scale, allows the derivation of local ( $\alpha$ ) diversity and turnover ( $\beta$ )  
368 relying on free to use and operationally available satellite data.

369 With regards to a potential validation with in-situ data, the uncertainty  
370 of wide-scale datasets hampers a spatial overlap. In this case, in-situ datasets

371 meet all five major concerns recently raised by Hobohm et al. (2019), i.e.:  
372 i) there is insufficient data coverage across Europe to make an unbiased  
373 comparison between predicted and actual distributions, ii) taxonomic stan-  
374 dards differ across sampled regions, iii) there are generally different shapes  
375 of areas being sampled, iv) political borders often define sampling areas and  
376 aggregated sampling areas, and v) data are not aggregated in the same way  
377 in all areas. Furthermore, spatial information has an intrinsic varying de-  
378 gree of relevance mainly due to the fact that, rather than species lists, it is  
379 composed of geometrical precision, attributes robustness and temporal con-  
380 sistency (Hobona et al., 2006). Finally, different models and approaches to  
381 measuring diversity inevitably provide different outputs, as pointed out in the  
382 generalised entropy theory put forward by Rényi (1961). Given the above  
383 validation difficulties, we decided to qualitatively compare our generated out-  
384 put, in particular the  $\beta$ -diversity map, with existing ecoregion maps, which  
385 are expected to discriminate different spatial areas based on natural bor-  
386 ders defined by biological diversity (<https://ecoregions2017.appspot.com/>)  
387 and thus are intrinsically related to differences in the species and spectral  
388 turnover of communities.

389 Since the output of the algorithm represents the variation of the pixel  
390 values in space and time, the most diverse pixels were those with the highest  
391 turnover among the neighborhood areas and most affected by seasonality.  
392 The importance of accounting for turnover instead of simple richness has  
393 been widely discussed in the ecological literature (Tuomisto, 2010), since  
394 environmental variability over spatial gradients is one of the major drivers  
395 of the structure and composition of diversity (Legendre et al., 2005). In this  
396 view, the use of the “spectral species concept”, defined as the variation of  
397 clustered pixel values, represents a powerful approach for the investigation  
398 of gradient variation of diversity in space and, potentially, in time.

399 In general, the measure of variability in space has been demonstrated  
400 to follow scale-based differentiation. In other words, results are expected  
401 to change with spatial scale in terms of both grain (spatial resolution) and  
402 extent (extent of geographical area of interest, Palmer et al. (2002)). Re-  
403 garding extent, one of the major weaknesses of the proposed algorithm in  
404  $\beta$ -diversity quantification (although this applies in general to all measure-  
405 ments of turnover) is that by increasing the extent of an observation area,  
406 the estimated values for an individual comparison between sites are modified  
407 by the increasing spectral species pool.

408 Additional drawbacks at the current stage of the algorithm include: i)  
409 the use of remotely sensed data which are not necessarily related to the main  
410 drivers of species distributions and of diversity, ii) the general multicollinear-  
411 ity found in most of the remotely sensed sets, iii) the unsupervised clustering

412 process being adopted.

413 Concerning climate, a solution might be found in the use of remotely  
414 sensed derived climate data adding climate change as an additional layer  
415 of complexity as in Rocchini et al. (2015a) and in (Zellweger et al., 2019).  
416 Also in this case multicollinearity of climate variables should be seriously  
417 taken into account, as we did for the original remote sensing data, by ap-  
418 plying a PCA to reduce the noise in the data and detect potential artifacts;  
419 consequently, PCA components might also be visualized to find potential  
420 congruence between spectral species and real species patterns. Finally, the  
421 process for grouping pixels in spectral species is based on an unsupervised  
422 clustering, where the definition of the number of clusters should be done a-  
423 priori. In this case, we hypothesized that the diversity of types of landscapes  
424 and gradient of climates across Europe may require a large number of clusters  
425 to correctly differentiate among them, relying on a fuzzy view of ecosystems  
426 (Rocchini and Ricotta, 2007). Hence, we decided to adopt a trial and error  
427 procedure until a threshold was reached in which no significant changes were  
428 found. Such a threshold resulted in 200 clusters. In the near future, it would  
429 be interesting to make a sensitivity analysis to demonstrate the impact of  
430 the number of clusters on the final analysis.

431 Considering the use of remote sensing for species diversity estimates, cor-  
432 relation and determination coefficients are generally statistically significant  
433 but low, hampering the direct use of remotely sensed diversity in simple uni-  
434 variate models (Rocchini et al., 2018). In fact, the relationship between  $\alpha$ -  
435 or  $\beta$ -diversity and habitat heterogeneity, which is the founding principle for  
436 the use of remote sensing data for these analyses, is rarely linear (Ferrier et  
437 al., 2007), mainly because of variation in the rate of species turnover along  
438 an environmental gradient. However, remotely sensed variables are generally  
439 well suited in more complex multivariate models accounting for part of the  
440 diversity explained for species communities (Rocchini et al., 2018). This is es-  
441 pecially true considering that environmental turnover generally explains more  
442 variation in species diversity rather than mere spatial structure (Hernandez-  
443 Stefanoni et al., 2012). Moreover, based on their high temporal resolution,  
444 remote sensing data might be useful to detect drastic changes of diversity  
445 in space and time, e.g. related to catastrophic events, overall considering  
446 the intrinsic difficulties in relying on in-situ data for wide geographical scales  
447 (Cord and Rödder, 2011; Hobohm et al., 2019).

448 From an ecological perspective, remote sensing imagery bands (dimen-  
449 sions) show a high affinity with the hypervolume axes proposed by Hutchin-  
450 son (1957) for modelling species niches. In the Hutchinson's theory, an hy-  
451 pervolume is represented by a space defined by a set of  $n$  independent axes  
452 which could be related to the final variables driving the realised niche of a

453 species (see also Blonder (2017) and Ricotta et al. (2010) on the niche dif-  
454 ferentiation concept). In our case, such axes would be the original satellite  
455 sensor bands being strictly related to the identification of a spectral species  
456 and the resulting spectral community in a site, instead of a niche. From this  
457 point of view, spectral species and communities are in line with joint species  
458 distribution models (JSDMs), which explicitly take into account biotic inter-  
459 actions among species in a community, while in our model the “interaction”  
460 among pixel values is ruled out in general by their proximity both from a  
461 spatial and from a spectral point of view. In this paper, the final aim was  
462 not to model single spectral species or spectral communities but rather to  
463 estimate diversity and its change over space and time, following the mathe-  
464 matical principles described in Liu et al. (2014) and Rocchini et al. (2015b),  
465 for which the distribution of diversity over space is actually a particular case  
466 of the so-called switched systems, i.e. hybrid systems resulting from both  
467 continuous and discrete dynamics with a high number of different poten-  
468 tial variables acting as main drivers of diversity response. In our view we  
469 succeeded here to fill a previous gap in spatio-ecological analysis, i.e. the  
470 translation of what in remote sensing science is known as “spectral mixture  
471 modeling” (Jensen, 2015) into an ecological diversity theory approach. In  
472 spectral mixture modeling the measured spectral reflectance is decomposed  
473 as a mixture of endmembers. In our case, such a mixture was used to di-  
474 rectly compute alpha- and beta-diversity over wide spatial areas in a very  
475 short time.

## 476 4 Conclusion

477 Predicting and mapping  $\alpha$ - and  $\beta$ -diversity using remotely sensed images ac-  
478 quired over large areas is currently a key topic in ecology, and could provide  
479 landscape managers with rapid and effective tools to estimate and monitor  
480 global change. In this paper, we proposed a novel method based on prelimi-  
481 nary unsupervised clustering of spectral data (NDVI time series derived from  
482 MODIS data), assigning each pixel to a “spectral species” and then calculat-  
483 ing diversity based on a dissimilarity metric. At the scale of this study, the  
484 one-to-one relationship between spectral species and in-situ plant species is  
485 not achieved, but the spectral species concept still holds true once consid-  
486 ering that the detected spectral species in the spectral space are related to  
487 higher-order plant hierarchies (assemblages, entire habitats, etc.). That is,  
488 from an algorithmic point of view, the bulk of the calculations are unaltered.

489 Based on the results presented here, the use of the spectral species and  
490 communities concept would appear to promote more effective planning and

491 policies related to the conservation of wild species, by improving our under-  
492 standing of the dynamics of local and global biodiversity at various spatial  
493 and temporal scales.

## 494 **5 Acknowledgements**

495 DR was partially supported by the H2020 project SHOWCASE and by the  
496 H2020 COST Action CA17134 “Optical synergies for spatiotemporal sensing  
497 of scalable ecophysiological traits (SENSECO)”. This paper has been par-  
498 tially developed during a Short Term Scientific Mission supported by the  
499 H2020 COST Action CA15212 “Citizen Science to promote creativity, scien-  
500 tific literacy, and innovation throughout Europe”.

501 JBF and FdB acknowledge financial support from Agence Nationale de  
502 la Recherche (BioCop project—ANR-17-CE32-0001) and TOSCA program  
503 grant of the French Space Agency (CNES) (HyperTropik/HyperBIO project).



## 504 References

- 505 Alados, C.L., Pueyo, Y., Escos, J., Andujar, A. (2009). Effects of the spatial  
506 pattern of disturbance on the patch-occupancy dynamics of juniper–pine  
507 open woodland. *Ecological Modelling*, 220: 1544-1550.
- 508 Asner, G.P. and Martin, R.E. (2009). Airborne spectranomics: mapping  
509 canopy chemical and taxonomic diversity in tropical forests. *Frontiers in*  
510 *Ecology and the Environment*, 7: 269-276.
- 511 Baselga, A. (2012). The relationship between species replacement, dissimilar-  
512 ity derived from nestedness, and nestedness. *Global Ecology and Biogeog-*  
513 *raphy* 21: 1223-1232.
- 514 Beierkuhnlein, C. (2003). Der Begriff Biodiversität. *Nova Acta Leopoldina*  
515 *N.F.*, 87: 51-72.
- 516 Blonder, B. (2017). Hypervolume concepts in niche- and trait-based ecology.  
517 *Ecography* 41: 1441-1445.
- 518 Borg, I., Groenen, P. (2005). *Modern Multidimensional Scaling: theory and*  
519 *applications* (2nd edition). Springer-Verlag, New York.
- 520 Bray, J.R. and Curtis J.T. (1957). An ordination of the upland forest com-  
521 munities of southern Wisconsin. *Ecological monographs* 27: 325-349.
- 522 Bruelheide, H., Dengler, J., Jimenez-Alfaro, B., Purschke, O., Hennekens,  
523 S.M., Chytrý, M., Pillar, V.D., Jansen, F., Kattge, J., Sandel, B., Aubin,  
524 I., Biurrun, I., Field, R., Haider, S., Jandt, U., Lenoir, J., Peet, R.K.,  
525 Peyre, G., Sabatini, F.M., Schmidt, M., Schrodte, F., Winter, M., Acic,  
526 S., Agrillo, E., Alvarez, M., Ambarlı, D., Angelini, P., Apostolova, I.,  
527 Arfin Khan, M.A.S., Arnst, E., Attorre, F., Baraloto, C., Beckmann, M.,  
528 Berg, C., Bergeron, Y., Bergmeier, E., Bjorkman, A.D., Bondareva, V.,  
529 Borchardt, P., Botta-Dukat, Z., Boyle, B., Breen, A., Brisse, H., Byun,  
530 C., Cabido, M.R., Casella, L., Cayuela, L., Cerny, T., Chepinoga, V.,  
531 Csiky, J., Curran, M., Custerovska, R., Dajic, Z., De Bie, S.E., de Ruffray,  
532 P., De Sanctis, M., Dimopoulos, P., Dressler, S., Ejrnaes, R., El-Rouf,  
533 M.A., El-Sheikh, M., Enquist, B., Ewald, J., Fagundes, J., Finckh, M.,  
534 Font, X., Forey, E., Fotiadis, G., Garcia-Mijangos, I., Luis de Gasper,  
535 A., Golub, V., Gutierrez, A.G., Hatim, M.Z., He, T., Higuchi, P., Hol-  
536 ubova, D., Holzner, N., Homeier, J., Indreica, A., Isik Gursoy, D., Jansen,  
537 S., Janssen, J., Jedrzejek, B., Jirousek, M., Jurgens, N., Kacki, Z., Kav-  
538 gacı, A., Kearsley, E., Kessler, M., Knollova, I., Kolomiychuk, V., Ko-  
539 rolyuk, A., Kozhevnikova, M., Kozub, L., Krstonosic, D., Kuhl, H., Kuhn,

540 I., Kuzemko, A., Kuzmic, F., Landucci, F., Lee, M.T., Levesley, A., Li,  
541 C.-F., Liu, H., Lopez-Gonzalez, G., Lysenko, T., Macanovic, A., Mahdavi,  
542 P., Manning, P., Marceno, C., Martynenko, V., Mencuccini, M., Minden,  
543 V., Moeslund, J.E., Moretti, M., Muller, J.V., Munzinger, J., Niinemets,  
544 U., Nobis, M., Noroozi, J., Nowak, A., Onyshchenko, V., Overbeck, G.E.,  
545 Ozinga, W.A., Pauchard, A., Pedashenko, H., Penuelas, J., Perez-Haase,  
546 A., Peterka, T., Pettrk, P., Phillips, O.L., Prokhorov, V., Rasomavicius,  
547 V., Revermann, R., Rodwell, J., Ruprecht, E., Rusina, S., Samimi, C.,  
548 Schaminee, J.H.J., Schmiedel, U., Sibik, J., Silc, U., Skvorc, Z., Smyth, A.,  
549 Sop, T., Sopotlieva, D., Sparrow, B., Stancic, Z., Svenning, J.-C., Swacha,  
550 G., Tang, Z., Tsiripidis, I., Turtureanu, P.D., Ugurlu, E., Uogintas, D.,  
551 Valachovic, M., Andre, K., Vashenyak, V.Y., Vassilev, K., Velez-Martin,  
552 E., Venanzoni, R., Vibrans, A.C., Violle, C., Virtanen, R., von Wehrden,  
553 H., Wagner, V., Walker, D.A., Wana, D., Weiher, E., Wesche, K., Whit-  
554 field, T., Willner, W., Wisser, S., Wohlgemuth, T., Yamalov, S., Zizka,  
555 G., Zverev, A. (2019). sPlot – a new tool for global vegetation analyses.  
556 *Journal of Vegetation Science*, 30: 161-186.

557 Chytry, M. , Hennekens, S. M., Jimenez-Alfaro, B. , Knollova, I. , Dengler, J.  
558 , Jansen, F. , Landucci, F. , Schaminee, J. H., Acic, S. , Agrillo, E. , Am-  
559 barli, D. , Angelini, P. , Apostolova, I. , Attorre, F. , Berg, C. , Bergmeier,  
560 E. , Biurrun, I. , Botta-Dukat, Z. , Brisse, H. , Campos, J. A., Carlon, L.  
561 , Carni, A. , Casella, L. , Csiky, J. , Custerevska, R. , Dajic Stevanovic,  
562 Z. , Danihelka, J. , De Bie, E. , Ruffray, P. , De Sanctis, M. , Dickore,  
563 W. B., Dimopoulos, P. , Dubyna, D. , Dziuba, T. , Ejrnæs, R. , Ermakov,  
564 N. , Ewald, J. , Fanelli, G. , Fernandez-Gonzalez, F. , FitzPatrick, U. ,  
565 Font, X. , Garcia-Mijangos, I. , Gavilan, R. G., Golub, V. , Guarino, R.  
566 , Haveman, R. , Indreica, A. , Isik GURSOY, D. , Jandt, U. , Janssen, J.  
567 A., Jirousek, M. , Kacki, Z. , Kavgacı, A. , Kleikamp, M. , Kolomiychuk,  
568 V. , Krstivojevic Cuk, M. , Krstonosic, D. , Kuzemko, A. , Lenoir, J. ,  
569 Lysenko, T. , Marcenò, C. , Martynenko, V. , Michalcova, D. , Moeslund,  
570 J. E., Onyshchenko, V. , Pedashenko, H. , Perez-Haase, A. , Peterka, T.  
571 , Prokhorov, V. , Rasomavicius, V. , Rodriguez-Rojo, M. P., Rodwell, J.  
572 S., Rogova, T. , Ruprecht, E. , Rusina, S. , Seidler, G. , Sibik, J. , Silc,  
573 U. , Skvorc, Z. , Sopotlieva, D. , Stancic, Z. , Svenning, J. , Swacha, G. ,  
574 Tsiripidis, I. , Turtureanu, P. D., Ugurlu, E. , Uogintas, D. , Valachovic,  
575 M. , Vashenyak, Y. , Vassilev, K. , Venanzoni, R. , Virtanen, R. , Weekes,  
576 L. , Willner, W. , Wohlgemuth, T., Yamalov, S. (2016), European Vegeta-  
577 tion Archive (EVA): an integrated database of European vegetation plots.  
578 *European Vegetation Archive (EVA): an integrated database of European*  
579 *vegetation plots. Applied Vegetation Science* 19: 173–180.

- 580 Cord, A., Rödder, D. (2011). Inclusion of habitat availability in species dis-  
581 tribution models through multi-temporal remote-sensing data? *Ecological*  
582 *Applications*, 21: 3285-3298.
- 583 Clark, J.S. (2008). Beyond neutral science. *Trends in Ecology and Evolution*,  
584 24: 8-15.
- 585 Currie, D.J. (1991). Energy and large-scale patterns of animal-and plant-  
586 species richness. *The American Naturalist* 137: 27-49.
- 587 Dinerstein, E., Olson, D., Joshi, A., Vynne, C., Burgess, N.D., Wikra-  
588 manayake, E., Hahn, N., Palminteri, S., Hedao, P., Noss, R., Hansen,  
589 M., Locke, H., Ellis, E.C., Jones, B., Barber, C.V., Hayes, R., Kormos,  
590 C., Martin, V., Crist, E., Sechrest, W., Price, L., Baillie, J.E.M., Wee-  
591 den, D., Suckling, K., Davis, C., Sizer, N., Moore, R., Thau, D., Birch,  
592 T., Potapov, P., Turubanova, S., Tyukavina, A., de Souza, N., Pintea, L.,  
593 Brito, J.C., Llewellyn, O.A., Miller, A.G., Patzelt, A., Ghazanfar, S.A.,  
594 Timberlake, J., Kloser, H., Shennan-Farpon, Y., Kindt, R., Lilleso, J.B.,  
595 van Breugel, P., Graudal, L., Voge, M., Al-Shammari, K.F., Saleem, M.A.  
596 (2017). Ecoregion-based approach to protecting half the terrestrial realm.  
597 *Bioscience*, 67: 534-545.
- 598 Elton, C.S. (1958). *The Ecology of invasions by animals and plants*. Methuen,  
599 London.
- 600 Ewald., M., Skowronek, S., Aerts, R., Dolos, K., Lenoir, J., Nicolas, M.,  
601 Warrie, J., Hattab, T., Feilhauer, H., Honnay, O., Garzon-Lopez, C.X.,  
602 Decocq, G., Van De Kerchove, R., Somers, B., Rocchini, D., Schmidlein,  
603 S. (2018). Analyzing remotely sensed structural and chemical canopy traits  
604 of a forest invaded by *Prunus serotina* over multiple spatial scales. *Biolog-*  
605 *ical Invasions*, 20: 2257-2271.
- 606 Féret, J.-B., Asner, G.P. (2014). Mapping tropical forest canopy diversity  
607 using high-fidelity imaging spectroscopy. *Ecological Applications* 24: 1289-  
608 1296.
- 609 Féret, J.-B., de Boissieu, F. (in press). **biodivMapR**: An R package for  $\alpha$ - and  
610  $\beta$ -diversity mapping using remotely sensed images. *Methods in Ecology*  
611 *and Evolution*.
- 612 Ferrier, S., Manion, G., Elith, J. and Richardson, K. (2007). Using gen-  
613 eralized dissimilarity modelling to analyse and predict patterns of beta  
614 diversity in regional biodiversity assessment. *Diversity and Distributions*  
615 13: 252-264.

- 616 Foody, G.M. (2008). GIS: biodiversity applications. *Progress in Physical Ge-*  
617 *ography* 32: 223-235.
- 618 Gaston, K.J. (2000). Global patterns in biodiversity. *Nature* 405: 220.
- 619 Gillespie, T.W., Foody, G.M., Rocchini, D., Giorgi, A.P. and Saatchi, S.  
620 (2008). Measuring and modelling biodiversity from space. *Progress in Phys-*  
621 *ical Geography* 32: 203-221.
- 622 Hernandez-Stefanoni, J.L., Gallardo-Cruz, J.A., Meave, J.A., Rocchini, D.,  
623 Bello-Pineda, J., Lopez-Martinez, J.O. (2012). Modeling alpha- and beta-  
624 diversity in a tropical forest from remotely sensed and spatial data. *Inter-*  
625 *national Journal of Applied Earth Observation and Geoinformation*, 19:  
626 359-368.
- 627 Hobbs, R.J., Arico, S., Aronson, J., Baron, J.S., Bridgewater, P., Cramer,  
628 V.A., Epstein, P.R., Ewel, J.J., Klink, C.A., Lugo, A.E., Norton, D.,  
629 Ojima, D., Richardson, D.M., Sanderson, E.W., Valladares, F., Vila, M.,  
630 Zamora, R., Zobel, M. (2006). Novel ecosystems: theoretical and man-  
631 agement aspects of the new ecological world order. *Global Ecology and*  
632 *Biogeography*, 15: 1-7.
- 633 Hobohm, C., Janisova, M., Steinbauer, M., Landi, S., Field, R., Vander-  
634 plank, S., Beierkuhnlein, C., Grytnes, J.-A., Vetaas, R.O., Fidelis, A., de  
635 Nascimento, L., Clark, V.P., Fernandez-Palacios, J.M., Franklin, S., Guar-  
636 ino, R., Huang, J., Krestov, P., Ma, K., Onipchenko, V., Palmer, M.W.,  
637 Fragomeni Simon, M., Stolz, C., Chiarucci, A. (2019). Global endemics-  
638 area relationships of vascular plants. *Perspectives in Ecology and Conser-*  
639 *vation*, 17, 41-49.
- 640 Hobona, G., James, P., Fairbairn, D. (2006). Multidimensional visualisation  
641 of degrees of relevance of geographic data. *International Journal of Geo-*  
642 *graphical Information Science*. 20: 469-490.
- 643 Hutchinson, G. (1957). Concluding remarks. *Cold Spring Harb. Symp.*  
644 *Quant. Biol.* 22: 415-427.
- 645 Jurasinski, G., Retzer, V., Beierkuhnlein, C. (2009). Inventory, differentia-  
646 tion, and proportional diversity: a consistent terminology for quantifying  
647 species diversity. *Oecologia*, 159: 15-26.
- 648 Jensen, R.J. (2015). *Introductory Digital Image Processing: A Remote Sens-*  
649 *ing Perspective*. Pearson Publishing.

- 650 Kohonen, T. (1982). Analysis of a simple self-organizing process. *Biological*  
651 *cybernetics* 44: 135-140.
- 652 Lande, R. (1996). Statistics and partitioning of species diversity, and simi-  
653 larity among multiple communities. *Oikos* 76: 5-13.
- 654 Legendre, P., Borcard, D., Peres-Neto, P.R. (2005). Analyzing beta diver-  
655 sity: partitioning the spatial variation of community composition data.  
656 *Ecological Monographs* 75: 435-450.
- 657 Liu, X., Zhong, S., Ding, X. (2014). A Razumikhin approach to exponential  
658 admissibility of switched descriptor delayed systems. *Applied Mathemati-*  
659 *cal Modelling* 38, 1647–1659.
- 660 Maldonado, C., Molina, C.I., Zizka, A., Persson, C., Taylor, C.M., Albán, J.,  
661 Chilquillo, E., Ronsted, N. and Antonelli, A. (2015). Estimating species  
662 diversity and distribution in the era of Big Data: to what extent can we  
663 trust public databases?. *Global Ecology and Biogeography* 24: 973-984.
- 664 Mead, A. (1992). Review of the Development of Multidimensional Scaling  
665 Methods. *The Statistician*, 41: 27-39.
- 666 Moran, P.A.P. (1950). Notes on continuous stochastic phenomena.  
667 *Biometrika*, 37: 17-23.
- 668 Mouchet, M., Levers, C., Zupan, L., Kuemmerle, T., Plutzer, C., Erb, K.,  
669 Lavorel, S., Thuiller, W., Haberl, H. (2015). Testing the effectiveness of  
670 environmental variables to explain European terrestrial vertebrate species  
671 richness across biogeographical scales. *PLoS ONE*, 10: e0131924.
- 672 Mucher, C.A., Hennekens, S.M., Bunce, R.G.H., Schaminee, J.H.J., Schaep-  
673 man, M.E. (2009). Modelling the spatial distribution of Natura 2000 habi-  
674 tats across Europe. *Landscape and Urban Planning*, 92: 148-159.
- 675 Palmer, M.W., Earls, P.G., Hoagland, B.W., White, P.S. and Wohlgemuth,  
676 T. (2002). Quantitative tools for perfecting species lists. *Environmetrics*,  
677 13: 121-137.
- 678 Peuquet, D.J. (1992). An algorithm for calculating minimum euclidean dis-  
679 tance between two geographic features. *Computers & Geosciences* 18: 989-  
680 1001.
- 681 R Development Core Team (2019). R: A Language and Environment for  
682 Statistical Computing. R Foundation for Statistical Computing, Vienna,  
683 Austria. <https://www.R-project.org/>

- 684 Rényi, A. (1961). On measures of information and entropy. Proceedings of  
685 the fourth Berkeley Symposium on Mathematics, Statistics and Probability  
686 1960: 547-561.
- 687 Ricotta, C., Godefroid, S., Rocchini, D. (2010). Patterns of native and exotic  
688 species richness in the urban flora of Brussels: rejecting the 'rich get richer'  
689 model. *Biological Invasions*, 12. 233-240.
- 690 Rocchini, D. (2007). Distance decay in spectral space in analysing ecosystem  
691  $\beta$ -diversity. *International Journal of Remote Sensing*, 28: 2635-2644.
- 692 Rocchini, D., Andreo, V., Förster, M., Garzon-Lopez, C.X., Gutierrez, A.P.,  
693 Gillespie, T.W., Hauffe, H.C., He, K.S., Kleinschmit, B., Mairota, P., Mar-  
694 cantonio, M., Metz, M., Nagendra, H., Pareeth, S., Ponti, L., Ricotta, C.,  
695 Rizzoli, A., Schaab, G., Zebisch, M., Zorer, R., Neteler, M. (2015a). Potential  
696 of remote sensing to predict species invasions: A modelling perspective.  
697 *Progress in Physical Geography*, 39: 283-309.
- 698 Rocchini, D., Balkenhol, N., Carter, G.A., Foody, G.M. Gillespie, T.W., He,  
699 K.S., Kark, S., Levin, N., Lucas, K., Luoto, M., Nagendra, H., Oldeland,  
700 J., Ricotta, C., Southworth, J. and Neteler, M. (2010). Remotely sensed  
701 spectral heterogeneity as a proxy of species diversity: recent advances and  
702 open challenges. *Ecological Informatics*, 5: 318-329.
- 703 Rocchini, D., Delucchi, L., Bacaro, G., Cavallini, P., Feilhauer, H., Foody,  
704 G.M., He, K.S., Nagendra, H., Porta, C., Ricotta, C., Schmidtlein, S.,  
705 Spano, L.D., Wegmann, M., Neteler, M. (2013). Calculating landscape  
706 diversity with information-theory based indices: A GRASS GIS solution.  
707 *Ecological Informatics*, 17: 82-93.
- 708 Rocchini, D., Luque, S., Pettorelli, N., Bastin, L., Doktor, D., Faedi, N.,  
709 Feilhauer, H., Féret, J.B., Foody, G.M., Gavish, Y., Godinho, S., Kunin,  
710 W.E., Lausch, A., Leitao, P.J., Marcantonio, M., Neteler, M., Ricotta,  
711 C., Schmidtlein, S., Vihervaara, P., Wegmann, M., Nagendra, H. (2018).  
712  $\beta$ -diversity by remote sensing: A challenge for biodiversity monitoring.  
713 *Methods in Ecology and Evolution* 9: 1787-1798.
- 714 Rocchini, D., Hernandez Stefanoni, J.L., He, K.S. (2015b). Advancing species  
715 diversity estimate by remotely sensed proxies: a conceptual review. *Eco-  
716 logical Informatics*, 25: 22-28.
- 717 Rocchini, D., McGlenn, D., Ricotta, C., Neteler, M., Wohlgemuth, T. (2011).  
718 Landscape complexity and spatial scale influence the relationship between



- 719 remotely sensed spectral diversity and survey based plant species richness.  
720 *Journal of Vegetation Science*, 22: 688-698.
- 721 Rocchini, D., Marcantonio, M., Da Re, D., Chirici, G., Galluzzi, M., Lenoir,  
722 J., Ricotta, C., Torresani, M., Ziv, G. (2019). Time-lapsing biodiversity:  
723 an open source method for measuring diversity changes by remote sensing.  
724 *Remote Sensing of Environment*, 231: 111192.
- 725 Rocchini, D., Ricotta, C. (2007). Are landscapes as crisp as we may think?  
726 *Ecological Modelling*, 204: 535-539.
- 727 Skowronek, S., Asner, G.P., Feilhauer, H. (2017). Performance of one-  
728 class classifiers for invasive species mapping using airborne imaging spec-  
729 troscopy. *Ecological Informatics*, 37: 66-76.
- 730 Skowronek, S., Ewald, M., Isermann, M., Van De Kerchove, R., Lenoir,  
731 J., Aerts, R., Warrie, J., Hattab, T., Honnay, O., Schmidtlein, S., Roc-  
732 chini, D., Somers, B., Feilhauer, H. (2017). Mapping an invasive bryophyte  
733 species using hyperspectral remote sensing data. *Biological Invasions*, 19:  
734 239-254.
- 735 Shannon, C.E. (1948). A mathematical theory of communication. *ACM SIG-*  
736 *MOBILE mobile computing and communications review* 5: 3-55.
- 737 Steinitz, O., Heller, J., Tsoar, A., Rotem, D., Kadmon, R. (2006). Environ-  
738 ment, dispersal and patterns of species similarity. *Journal of Biogeography*:  
739 33, 1044-1054.
- 740 Sun, L., Mi, X., Wei, J., Wang, J., Tian, X., Yu, H. and Gan, P. (2017). A  
741 cloud detection algorithm-generating method for remote sensing data at  
742 visible to short-wave infrared wavelengths. *ISPRS Journal of Photogram-*  
743 *metry and Remote Sensing* 124: 70-88.
- 744 Tobler, W., (1970). A computer movie simulating urban growth in the Detroit  
745 region. *Economic Geography*, 46: 234-240.
- 746 Tuanmu, M.N., Jetz, W. (2015). A global, remote sensing-based character-  
747 ization of terrestrial habitat heterogeneity for biodiversity and ecosystem  
748 modelling. *Global Ecology and Biogeography*, 24: 1329-1339.
- 749 Tuomisto, H. (2010). A consistent terminology for quantifying species diver-  
750 sity? Yes, it does exist. *Oecologia* 164: 853-860.
- 751 Ustin, S.L. and Gamon, J.A. (2010). Remote sensing of plant functional  
752 types. *New Phytologist* 186.4: 795-816.

- 753 Vihervaara, P., Auvinen, A.P., Mononen, L., Torma, M., Ahlroth, P., Anttila,  
754 S., Bottcher, K., Forsius, M., Heino, J., Heliola, J., Koskelainen, M., Kuus-  
755 saari, M., Meissner, K., Ojala, O., Tuominen, S., Viitasalo, M., Virkkala,  
756 R. (2017). How Essential Biodiversity Variables and remote sensing can  
757 help national biodiversity monitoring. *Global Ecology and Conservation*,  
758 10: 43-59.
- 759 Waples, R., Gaggiotti, O. (2006). What is a population? An empirical eval-  
760 uation of some genetic methods for identifying the number of gene pools  
761 and their degree of connectivity. *Molecular Ecology*, 15: 1419-1439.
- 762 Wegmann, M., Leutner, B. and Dech, S. eds. Remote sensing and GIS for  
763 ecologists: using open source software. (2016). Pelagic Publishing Ltd,  
764 2016.
- 765 Whittaker, R.H. (1972). Evolution and measurement of species diversity.  
766 *Taxon* 21: 213-251.
- 767 Zellweger, F., De Frenne, P., Lenoir, J., Rocchini, D., Coomes, D. (2019).  
768 Advances in microclimate ecology arising from remote sensing. *Trends in*  
769 *Ecology & Evolution*, 34: 327-341.

770 **Figures**

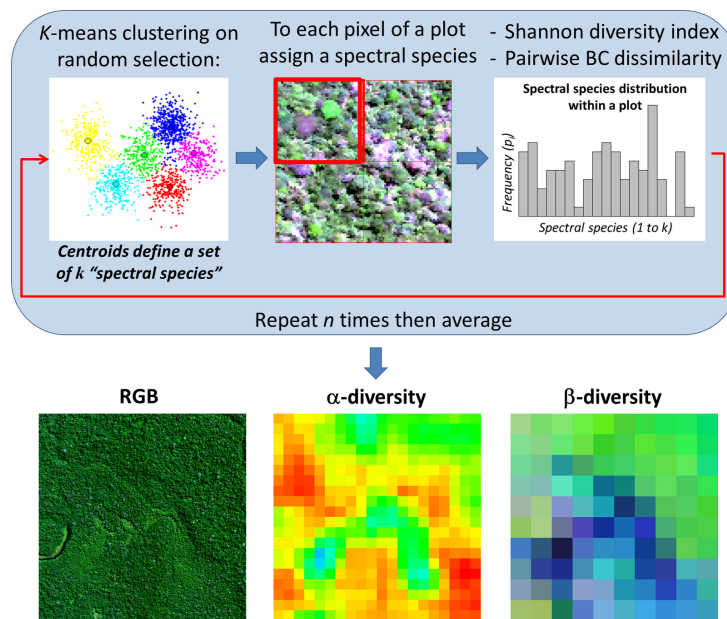


Figure 1: Diagrammatic representation of the steps of the algorithm used to achieve  $\alpha$ - and  $\beta$ -diversities, redrawn from (Féret and Asner, 2014). Pixels are clumped in a spectral species and spectral community diversity is calculated. We refer to the main text and to Box 1 for additional information.

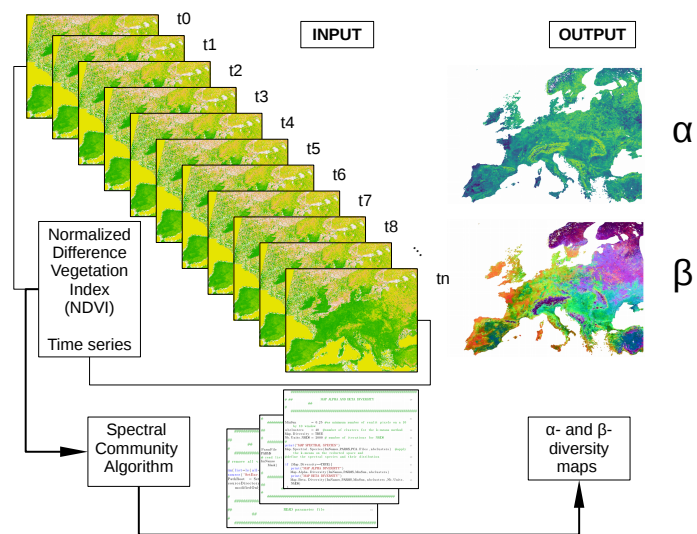


Figure 2: An input set of  $n$  images can be handled to create a time series and use the stack to further calculate the spectral community diversity. In our paper, a stack of 12 NDVI images of 2018 from the MODIS sensor was processed by the spectral species algorithm, by producing  $\alpha$ - and  $\beta$ -diversity maps.

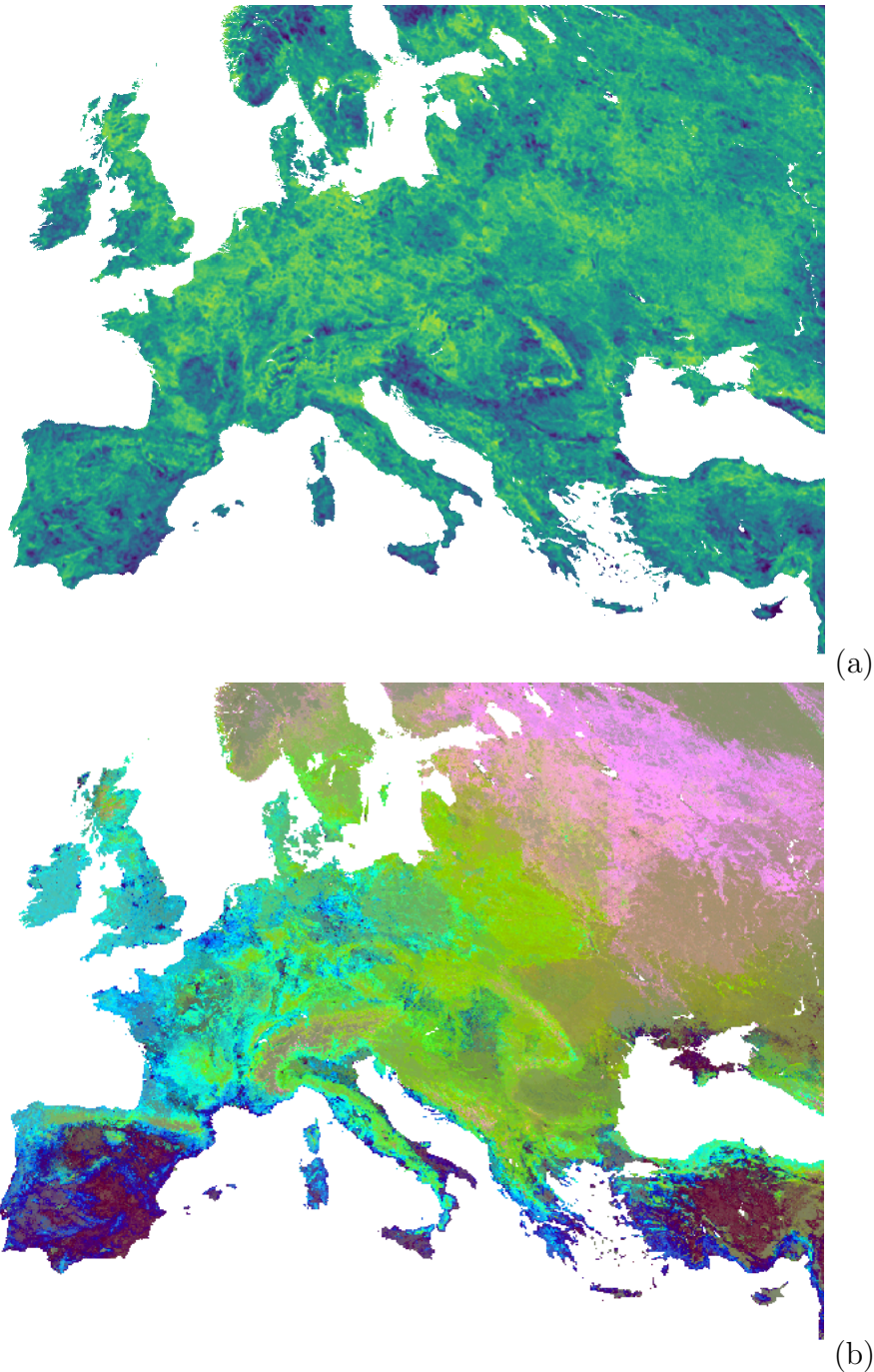


Figure 3:  $\alpha$ - (a) and  $\beta$ -diversity (b) maps obtained by the spectral species algorithm. (a) The  $\alpha$ -diversity map, based on Shannon's  $H'$  index (ranging from blue [low values] to light green [high values]) calculated in a 10x10 pixels local neighbourhood, corresponds to the local entropy of clusters, so that each location is independent from the others; (b) The  $\beta$ -diversity map - Bray-Curtis dissimilarity reduced to 3 dimensions with NMDS - provides information about the dissimilarity along any location in the image. Here, the distance between pairs of spatial units is expressed as a 3 colour code.



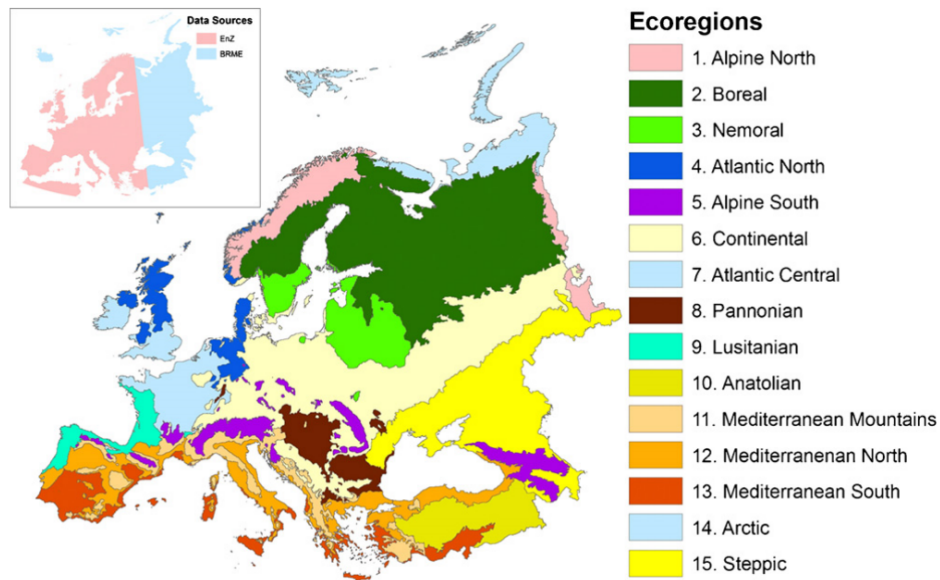


Figure 4: European Environmental Agency ecoregions map redrawn by Mucher et al. (2009). Similar maps at a coarser grain are provided by Mouchet et al. (2015) and Dinerstein et al. (2017).

---

771 **Box 1 - Steps composing the spectral species**  
772 **algorithm**

---

- 773 1. A Principal Component Analysis (PCA) is applied to the spectral data.  
774 PCA is not performed on the whole image, but only on a large subset  
775 of pixels randomly selected from the image. Due to the high dimen-  
776 sionality of the data, the reduction of the dataset is not altering the  
777 result. Those principal components explaining most of the variance of  
778 the original set are then retained for further steps.
- 779 2. A subset of pixels is then randomly selected across the entire map and  
780 the spectral space containing such a subset is partitioned into spectral  
781 species using k-means clustering with the number of k clusters being  
782 decided a priori. Then the centroids defining the spectral species are  
783 located.
- 784 3. The spectral dataset is divided into final mapping units. Each pixel  
785 is assigned to a given spectral species based on the minimal Euclidean  
786 distance between pixels (Peuquet, 1992) and the previously defined  
787 centroids.
- 788 4. A spectral species distribution is obtained for each mapping unit from  
789 which the  $\alpha$ - and  $\beta$ -diversity indices are computed as previously stated.
- 790 5. Since the spectral species distribution is obtained by a subset of pixels,  
791 in order to avoid under-representation of some small-scaled ecological  
792 classes (e.g. small scale vegetation patterns), steps 4 and 5 are repeated  
793 100 times, and the indicators obtained for each repetition are averaged.  
794 In particular the Bray-Curtis dissimilarity matrix is computed for each  
795 pair of spatial units, based on their spectral species distribution at each  
796 iteration; then the final matrix corresponds to the BC dissimilarity  
797 averaged over all the iterations.
- 798 6. Non metric Multidimensional Scaling (NMDS) (e.g. Borg and Groenen  
799 (2005)) is applied to the matrices in order to obtain a visual representa-  
800 tion of the results. NMDS is an ordination technique usually applied in  
801 ecology that differs from other ordination techniques as PCA, since in  
802 NMDS a small number of axes are chosen prior to the analysis and then  
803 the data are fitted into the chosen dimensions. Furthermore, NMDS

804 is not an analytical but numerical technique, seeking for the right so-  
805 lution (convergence) iteratively. Finally, NMDS is not an eigenvector-  
806 eigenvalue technique, hence a NMDS ordination can be rotated among  
807 the axes. NMDS is mostly used in ecology for its versatility since it  
808 accepts any distance measure of the samples. In this case the Bray-  
809 Curtis matrix was used. In the applied NMDS approach, the first step  
810 is generally to decide the number of reduced dimensions; in this case  
811 3 dimensions were chosen. The algorithm starts with the construction  
812 of initial random arrangements of the pixels. Then the Euclidean dis-  
813 tances among the samples is calculated in this first configuration; those  
814 distances are regressed against the original distance matrix, and the  
815 predicted ordination distances are calculated. Finally, the regression is  
816 fitted by the least-squares method. The goodness of fit is measured by  
817 the sum of squared differences between ordination-based distances and  
818 the predicted distances. The goodness of fit is calculated through the  
819 Kruskal's Stress index:

$$Stress = \sqrt{\frac{[r]\sum_{h,i}(d_{hi} - \hat{d}_{hi})^2}{[r]\sum_{h,i}d_{hi}^2}} \quad (3)$$

820 where  $d_{hi}$  is the ordinated distance between pixels  $h$  and  $i$ , and  $\hat{d}_{hi}$  is the  
821 distance predicted from the regression. Then, a new configuration is  
822 computed moving in the direction in which stress changes most rapidly.  
823 The entire procedure is repeated until convergence. A *Stress* value  
824 that provides an excellent representation in the reduced dimensions is  
825 considered to be lower than 0.05; nevertheless a value of *Stress* < 0.2  
826 is still considered a good representation Borg and Groenen (2005).

827 Basically, the algorithm provides both single spectral species maps and  
828 the  $\alpha$ - and  $\beta$ -diversity maps. The algorithm input file needs to be in ENVI  
829 binary format with the corresponding header file. The file should be in Band  
830 Interleave by Line (BIL) format and 2-byte signed integer, and should not  
831 have extension. A further masking file in the same format is necessary in  
832 order to mask clouds and water surfaces.

---

833 **Box 2 - Packages used in this manuscript to**  
834 **handle and analyse spatial data in R**

---

- 835 • **raster**: It provides classes and functions to manipulate geographic  
836 data in raster format. Raster data divides space into cells (as pixels) of  
837 equal size (in units of the coordinate reference system). Along with the  
838 **raster** package, the **sp** package is also loaded, which provides spatial  
839 object classes and methods to retrieve coordinates.
  - 840 • **rgdal**: It provides functions to import and export spatial data in differ-  
841 ent formats.
  - 842 • **RStoolbox**: A toolbox for remote sensing image processing and analy-  
843 sis.
  - 844 • **rasterdiv**: It provides algorithms for measuring diversity from spatial  
845 matrices.
-